



1 **Measurement Report: Wintertime new particle formation in the rural area of North**
2 **China Plain: influencing factors and possible formation mechanism**

3
4

5 **Juan Hong^{1,2†*}, Min Tang^{1,2†}, Qiaoqiao Wang^{1,2*}, Nan Ma^{1,2}, Shaowen Zhu^{1,2}, Shaobin**
6 **Zhang^{1,2}, Xihao Pan^{1,2}, Linhong Xie^{1,2}, Guo Li³, Uwe Kuhn³, Chao Yan⁴, Jiangchuan**
7 **Tao^{1,2}, Ye Kuang^{1,2}, Yao He^{1,2}, Wanyun Xu⁵, Runlong Cai⁶, Yaqing Zhou^{1,2}, Zhibin Wang⁷,**
8 **Guangsheng Zhou⁵, Bin Yuan¹, Yafang Cheng³, Hang Su³**

9

10 ¹Institute for Environmental and Climate Research, Jinan University, Guangzhou, Guangdong
11 511443, China

12 ²Guangdong-Hongkong-Macau Joint Laboratory of Collaborative Innovation for Environmental
13 Quality, Guangzhou, China

14 ³Multiphase Chemistry Department, Max Planck Institute for Chemistry, Mainz 55128, Germany

15 ⁴School of Atmospheric Sciences, Joint International Research Laboratory of Atmospheric and
16 Earth System Sciences, Nanjing University, Nanjing, China

17 ⁵Hebei Gucheng, Agrometeorology, National Observation and Research Station, Chinese Academy
18 of Meteorological Sciences, Beijing, 100081, China

19 ⁶Institute for Atmospheric and Earth System Research/Physics, Faculty of Science, University of
20 Helsinki, Helsinki, FI00014, Finland

21 ⁷College of Environmental and Resource Sciences, Zhejiang University, Zhejiang Provincial Key
22 Laboratory of Organic Pollution Process and Control, Hangzhou 310058, China

23 [†]These authors contributed equally to this work.

24 ^{*}Correspondence: Qiaoqiao Wang (qwang@jnu.edu.cn) and Juan Hong
25 (juanhong0108@jnu.edu.cn)

26

27 **Abstract:**

28 The high concentration of fine particles as well as gaseous pollutants makes
29 polluted areas, such as the urban setting of North China Plain (NCP) of China, a
30 different environment for NPF compared to many clean regions. Such conditions also
31 hold for other polluted environments in this region, for instance, the rural area of NCP,
32 yet the underlying mechanisms for NPF remain less understood owing to the limited
33 observations of particles in the sub-3nm range. Comprehensive measurements,
34 particularly covering the particle number size distribution down to 1.34 nm, were
35 conducted at a rural background site of Gucheng (GC) in the North China Plain (NCP)
36 from 12 November to 24 December in 2018. Five NPF events during the 39 effective
37 days of measurements for the campaign were identified, with the mean particle



38 nucleation rate ($J_{1,34}$) and growth rate ($GR_{1,34-2,4}$) were $29.1 \text{ cm}^{-3}\cdot\text{s}^{-1}$ and $0.54 \text{ nm}\cdot\text{h}^{-1}$,
39 respectively. During these five days, NPF concurrently occurred in an urban site in
40 Beijing, indicating that NPF events during these days in this region might be a regional
41 phenomena. This implies that H₂SO₄-amine nucleation, concluded for urban Beijing
42 there, could also be the dominating mechanism for NPF at our rural site. The
43 condensation sink or coagulation sink for the survival of newly-formed and small
44 clusters are the dominating factor controlling the occurrence of NPF under current
45 atmosphere, whereas the contribution from the available H₂SO₄ cannot be neglected,
46 either. This feature is slightly different from that of urban Beijing, where CS mainly
47 determines whether NPF takes place or not.

48

49 **Keywords:** new particle formation, particle number size distribution, condensation
50 sink, nucleation mechanism.



51 1. Introduction

52 Atmospheric new particle formation (NPF) is a major source of the global particles
53 in terms of number concentration and size distribution (Kulmala et al., 2004) and is
54 considered to contribute up to half of the global cloud condensation nuclei (CCN)
55 budget in the lower troposphere (Spracklen et al., 2006; Dunne et al., 2016). In general,
56 NPF consists of two consecutive processes: a) the formation or nucleation of molecular
57 clusters by low-volatile gaseous substances, and b) their subsequent growth to
58 detectable sizes or even larger, at which these particles may act as CCNs or contribute
59 to the particle mass concentration (Kulmala et al., 2000; Zhang et al., 2012).

60 Numerous laboratory measurements and field studies have shown that sulfuric
61 acid (H_2SO_4) are the key precursors to form molecular clusters for nucleation
62 (Nieminen et al., 2010; Sipilä et al., 2010; Kirkby et al., 2011; Riccobono et al., 2014;
63 Stolzenburg et al., 2020). However, these H_2SO_4 clusters relevant to atmospheric
64 nucleation are typically quite small, i.e., with diameters below 1.5 nm, at which the
65 detection efficiency of traditional instruments specific for NPF was usually
66 unsatisfactory (Kulmala et al., 2013). This had led to large uncertainties in the
67 measured formation rate of newly-formed particles and thus required precise
68 measurements of these clusters or particles down to sub-3 nm. Upon recently,
69 progress such as the use of a particle size magnifier (PSM) (Vanhanen et al., 2011; Xiao
70 et al., 2015), a neutral cluster and air ion spectrometer (NAIS) (Pushpawela et al., 2019;
71 Sulo et al., 2020) and a chemical ionization atmospheric pressure interface time of-
72 flight mass spectrometer (CI-API-TOF) (Kürten et al., 2016; Sulo et al., 2020) make it
73 possible to directly measure the number concentration as well as the chemical
74 composition of clusters in the 1-3 nm size range. Benefit from these novel techniques,
75 observations have found that the growth of H_2SO_4 clusters would be significantly
76 promoted after stabilized by other precursors like amines, ammonia or iodine species
77 (Berndt et al., 2010; Kirkby et al., 2011; Almeida et al., 2013; Riccobono et al., 2014;
78 Kürten et al., 2016; Sipilä et al., 2010). Furthermore, oxidation products from volatile



79 organic compounds, for instance, highly oxidized organic compounds, were suggested
80 to be important contributors participating in atmospheric nucleation (Ehn et al., 2014;
81 Bianchi et al., 2016; Kirkby et al., 2016; Tröstl et al., 2016).

82 The North China Plain (NCP) of China, has been suffering heavily from the highly
83 complex air pollution since decades (Ma et al., 2016; Shen et al., 2018; Zhang et al.,
84 2020), owing to the high emissions or formations of different pollutants such as SO₂,
85 NH₃, VOCs as well as fine particles from various sources (Guo et al., 2014; Zhang et al.,
86 2015). Due to the high concentration of pre-existing particles, previous studies
87 considered that in the NCP, less NPF would occur as the newly-formed particles would
88 be scavenged much faster before growing. By contrast, atmospheric NPF was still
89 frequently observed in this region (Chu et al., 2019; Deng et al., 2020; Cai et al., 2021),
90 being more often than theoretically predicted (Kulmala et al., 2014), indicating that
91 the underlying mechanisms for NPF in this area might be different, that those
92 mechanism previously found for other environments might not be completely
93 applicable. The higher concentration of these gaseous precursors makes this region an
94 unique condition for NPF compared to relatively clean environments (Kulmama et al.,
95 2016; Yu et al., 2017; Wang et al., 2017), further supporting the hypothesis of different
96 formation mechanisms and thereby distinct features of NPF events in this region.
97 These doubts concerning NPF in the NCP, however, still remain to be elucidated due to
98 limitations of comprehensive measurements, particularly for rural areas of the NCP,
99 where observations regarding NPF was even more rare.

100 In addition, with respect to those existing studies concerning NPF in the NCP, they
101 mainly focused on the measurements of particles beyond 3 nm. Without applicable
102 instruments, observations of new particles down to sub-3nm was still quite limited
103 (Fang et al., 2020; Zhou et al., 2020), causing large uncertainties in the measured
104 characteristics of NPF for current region. To fill the gap of measurements of particles
105 or clusters in the size range of 1-3 nm and further advance our understanding of NPF
106 in this region, particularly in the rural area of NCP, we conducted a comprehensive
107 measurement campaign at a rural background site in the NCP during November 12 to
108 December 24, 2018. By obtaining the particle number size distribution over a wide



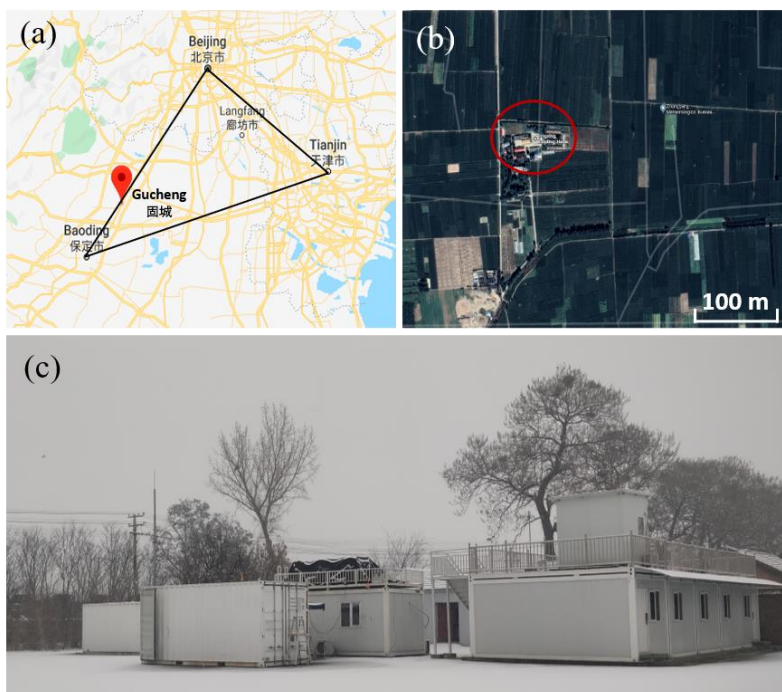
109 diameter range (1.34 nm - 10 μ m), we aimed to investigate the characteristics of NPF
110 events at the rural site in NCP during wintertime, find out which factors govern the
111 occurring of NPF compared to other regions of NCP such as the urban areas and
112 explore the potential mechanisms for NPF in this area.



113 2. Experiment

114 2.1. Field measurements site

115 The measurements were conducted at Gucheng (GC) site ($39^{\circ}09'01.1''\text{N}$
116 $115^{\circ}44'02.6''\text{E}$), situated at an Ecological and Agricultural Meteorology Station ($39^{\circ}09'$
117 N , $115^{\circ}44' \text{E}$) of the Chinese Academy of Meteorological Sciences from 12 November
118 to 24 December in 2018. The station is located in Dingxing county, Baoding city, Hebei
119 Province, China, as seen in Fig.1 and surrounded by agricultural fields and sporadic
120 villages. Being far from the urban and industrial emission areas, this site can be treated
121 as a representative regional site in the northern part of NCP. More details about this
122 site can be found in Lin et al. (2009) and Shen et al. (2018).



123
124 Figure 1. The upper panel shows the geographical location of the site (red dot and circled, ©
125 Google Maps), where our field measurements were carried out. The lower panel shows the
126 measurement containers, where the sampling instruments were set up.



127 **2.2. Measurements**

128 **2.2.1. Particle Number Size Distribution (PNSD) measurement**

129 The aerosol sampling inlet was located on the rooftop of a measurement
130 container, where room temperature was maintained at 22 °C (Fig1. c). The aerosol was
131 sampled via a low-flow PM10 cyclone inlet, passed through a Nafion dryer, and
132 directed to different instruments through stainless steel or conductive black tubings
133 using an isokinetic flow splitter. The particle number size distribution of aerosol
134 particles with diameters from 10 nm to 10000 nm was measured by using a scanning
135 mobility particle sizer (SMPS, model TSI 3938) and an Aerodynamic Particle Size
136 Spectrometer (APS, model TSI 3321) at a time resolution of around 5 minutes. The
137 SMPS consisted of an electrostatic classifier (model TSI 3080), a differential mobility
138 analyzer (DMA, model TSI 3081) and a condensation particle counter (CPC, model TSI
139 3772).

140 **2.2.2. Sub-3nm Particle Number Concentration measurement**

141 Sub-3nm particles were measured with an Airmodus nano Condensation Nucleus
142 Counter system (nCNC, model A11), consisting of a Particle Size Magnifier (PSM, model
143 A10) and a butanol condensation particle counter (CPC, model A20) (Kangasluoma et
144 al., 2016). The Airmodus PSM uses diethylene glycol as the working fluid to activate
145 and grow nano-sized particles. Specifically, the PSM was operated under the scanning
146 mode that the diethylene glycol flow was varied between 0.1 to 1.3 L·min⁻¹. Thus, the
147 number size distribution of five different size bins, i.e., 1.34-1.39, 1.39-1.60, 1.60-1.94,
148 1.94-2.40, and 2.40-3.70 nm was obtained. Owing to the data quality, only the former
149 four size bins data were used in this study. During this campaign, the duration of each
150 scan was completed within around 240 s.

151 **2.2.3. Pollutant gases, PM2.5 and meteorological parameters measurement**

152 Concentration of trace gases, including SO₂, O₃, CO and NO_x, was measured



153 continuously during this campaign using different Thermo Fisher Analyzers (model 43i-
154 TLE, 49i, 48i, and 42i), respectively, at a time resolution of 1 minute. The non-refractory
155 submicron aerosol chemical composition was measured by an Aerosol Chemical
156 Speciation Monitor (ACSM, Aerodyne, USA) (Sun et al., 2012) and the black carbon
157 mass concentration was measured by a 7-wavelength aethalometer (model AE-33,
158 Magee Scientific Inc., USA) (Petzold et al., 2013) using a PM2.5 inlet.

159 In addition, ambient meteorological conditions, such as wind speed, wind
160 direction, temperature, relative humidity and solar radiation, were also regularly
161 measured in another building, which is located about 20 meters to the southwest of
162 the container, at the same observational site.

163 2.3. Data processing

164 2.3.1. Formation Rate (J_{D_p}) and Growth Rate (GR)

165 J_{D_p} defines the formation rate of atmospheric particles at a certain diameter (D_p)
166 and can be calculated according to Kulmala et al. (2012) as:

$$167 \quad J_{D_p} = \frac{dN_{\Delta D_p}}{dt} + CoagS_{\Delta D_p} \times N_{\Delta D_p} + \frac{1}{\Delta D_p} GR_{\Delta D_p} \times N_{\Delta D_p}$$

168 where N is the particle number concentration between the diameter dp_2 and dp_1
169 (denotes as ΔD_p), $CoagS$ is the coagulation sink of particles, GR is the particle
170 growth rate out of the selected size bin.

171 In our study, we used two independent methods to calculate GR. One is the
172 maximum concentration method (Kulmala et al., 2012), being mainly for PSM data.
173 The other is based on the variation in geometric mean diameters of particle number
174 size distribution, which is derived by fitting the PNSD into 2 or 3 log-normal modes
175 using an automatic algorithm (DO-FIT model) (Hussein et al., 2005), mainly for SMPS
176 data.

$$177 \quad GR = \frac{ddp}{dt} = \frac{\Delta dp}{\Delta t} = \frac{dp_2 - dp_1}{t_2 - t_1}$$

178 where dp_1 and dp_2 were particle diameters at time t_1 and t_2 , respectively.



179 2.3.2. Condensation Sink (CS) and Coagulation Sink (CoagS)

180 CS describes how fast the low-volatility molecules condense onto pre-existing
181 aerosols and can be expressed as (Kulmala et al., 2012):

$$182 \quad CS = 2\pi D \int_0^{dp_{max}} \beta_{m,dp} dp N_{dp} ddp = 2\pi D \sum_{dp} \beta_{m,dp} dp N_{dp}$$

183 where D is the diffusion coefficient of the condensing vapor, which is usually referred
184 to sulfuric acid and $\beta_{m,dp}$ is the mass flux transition correction factor.

185 CoagS represents how fast the fresh formed particles are lost to pre-existing
186 particles through coagulation and can be calculated as :

$$187 \quad CoagS_{dp} = \int K(dp, dp') n(dp) ddp' \cong \sum_{dp'=dp}^{dp'=max} K(dp, dp') N_{dp'}$$

188 where, $K(dp, dp')$ is the collision efficiency between particles at the diameter
189 from dp to dp' .

190 2.3.3. Sulfuric Acid proxy (SA proxy)

191 SA was considered as one of the key precursors responsible for particle nucleation
192 in the atmosphere. However, no direct measurement for the concentration of SA was
193 available in current study. We therefore used a proxy variable to substitute the
194 concentration of SA, as SA is mainly produced by the oxidation of SO₂ by OH radicals,
195 which can be approximated by the UV-B intensity (Petäjä et al., 2009). Thus, the proxy
196 concentration of SA can be calculated by (Zhu et al., 2017):

$$197 \quad SA \text{ proxy} = k \cdot \frac{[SO_2] \cdot SR}{CS}$$

198 where, k is a scaling constant and was assumed to be $2.3 \times 10^{-9} \text{ m}^2 / (\text{W}\cdot\text{s})$.

199 2.3.4. Classification of NPF event

200 Days of NPF events was classified according to the method proposed by Dal Maso
201 et al. (2005) and Kulmala et al. (2012), in which (a) a new particle mode appears from
202 the particle number size distribution within the nucleation mode size range, (b) the



203 particles in new mode prevail and have a continuous growth over a time span of hours.
204 In addition to the traditional classification for NPF, a burst in sub-3nm particles or
205 clusters and subsequent growth to larger size for a few hours that was visually available
206 from PSM data was also considered as an NPF event.



207 **3. Results and discussions**

208 **General characteristics of NPF at GC site**

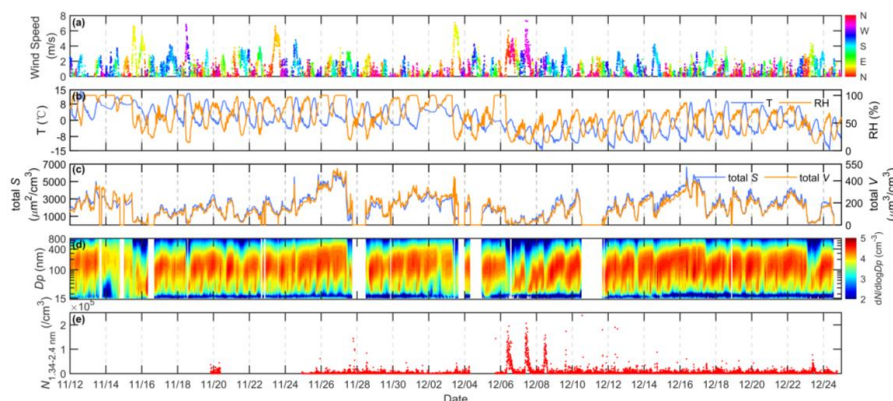
209 Figure 2 shows the time series of meteorological parameters (a: wind speed and
210 direction, b: temperature and relative humidity) and aerosol properties (c: total
211 surface and volume concentration, d and e: PNSD in the size range of 10 to 800 nm
212 and particle number concentration in the range of 1.34 to 2.40 nm) during this field
213 campaign. During our study, wind speed was typically quite low with an average of
214 $1.18 \text{ m}\cdot\text{s}^{-1}$, indicating stagnant meteorological conditions for the limited dilution of air
215 pollutants at current site. The temperature and relative humidity (RH) show opposite
216 diurnal variation over the observational period, with the highest temperature and
217 lowest RH during daytime and vice versa during nighttime.

218

219 According to the PNSD and PSM data, five days, with three of which having significant
220 burst of sub-3 nm clusters as shown in Fig.2e, were classified as NPF event out of the
221 total experimental period. This corresponds to an NPF frequency of 12.8%, which was
222 lower compared to those at an urban site (ie., Beijing) in the same region during the
223 same season (Shen et al. (2018) (25.8%); Deng et al. (2020) (51.4%)). Similar findings
224 were also observed in Yue et al. (2009) and Wang et al. (2013), that NPF frequencies
225 were higher at the Beijing urban site than at the corresponding regional background
226 or rural site. They attributed this to the higher pollution level and correspondingly
227 higher precursor content in the urban cities, leading to stronger NPF events there.

228

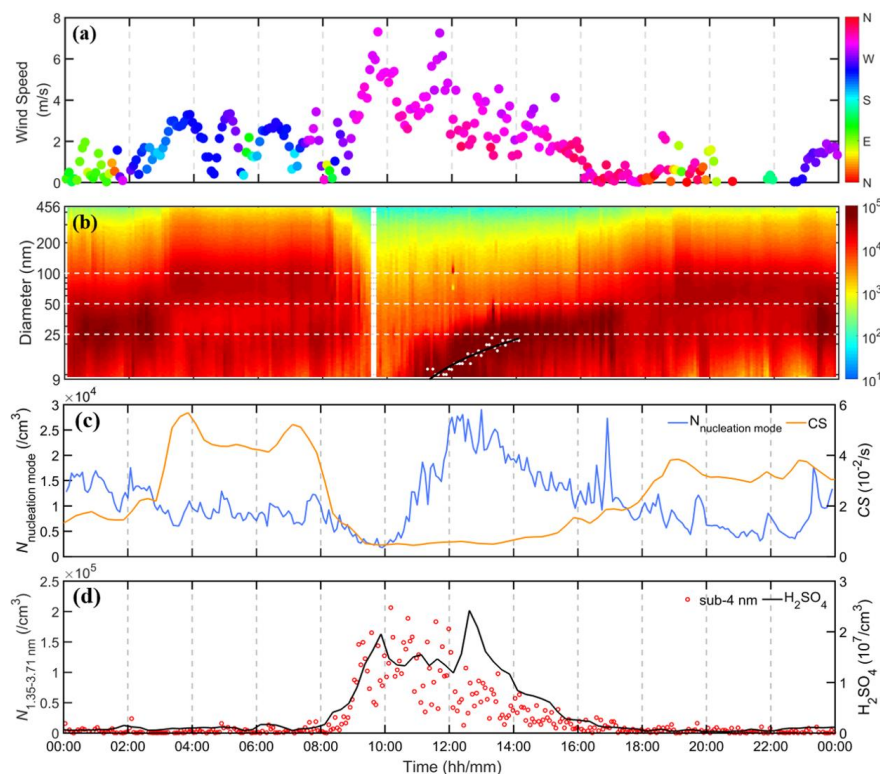
229



230
231 **Figure 2.** Time series of (a) wind speed and wind direction, (b) temperature (T) and relative
232 humidity (RH), (c) total particle surface and volume concentration calculated by using PNSD data,
233 (d) measured PNSD in the size range of 10 - 800 nm, (e) particle number concentration in the range
234 of 1.34 to 2.40 nm during the entire measurement period (2018.11.12-2018.12.24). White portion
235 indicates no data was available due to instrument maintenance or power failure.

236

237 Figure 3 shows a typical NPF event on December 7 as an example. Northwest wind
238 prevailed with elevated wind speed starting from around 8:00 o'clock, which was
239 conducive to the diffusion of local pollutants, leading to a dramatic decrease in CS
240 concurrently. At the same time, an obvious rise in H_2SO_4 concentration was observed,
241 coinciding with a strong burst in the concentration of sub-3 nm clusters. Then, new
242 particles with diameter larger than 10 nm, as shown in Fig. 3b, gradually formed by
243 growth, exhibited as a visible banana shape in PNSD.



244

245 **Figure 3.** A case of NPF event on December 7 during this field campaign. Time series of (a) wind
246 speed and wind directions, (b) the PNSD in the size range of 9-400 nm (The white dotted line
247 represents the size with diameter at 25, 50, and 100 nm; black line represents the polynomial fit
248 of the measured PNSD, (c) the particle number concentration of nucleation mode (9-25nm) and CS,
249 (d) the number concentration of sub-3nm clusters and predicted concentration of sulfuric acid.

250

251 For all the identified NPF events, the formation rate of 1.34 nm ($J_{1.34}$) particles ranged
252 from 8.01 cm⁻³·s⁻¹ to about 40.8 cm⁻³·s⁻¹ with an average value of 29.1 cm⁻³·s⁻¹ at our
253 GC site during the measurement period. It has to be noted that most atmospheric
254 formation rate reported in China was based on the measured formation rate at
255 relatively larger size, i.e., 3-10 nm. However, according to Chu et al. (2019), large errors
256 may associate with the deviations of J when using data at larger sizes as GR at sub-3
257 nm is needed but were typically unclear. Therefore, we focused more on the formation
258 rate of particles at sizes below 3 nm in the following discussion. In principle, particle
259 formation rate is inversely proportional to the CS, as the nucleation precursors or



260 clusters would be scavenged more rapidly under higher CS conditions, leading to a
261 slower nanoparticle formation with a lower J . However, as shown in Table 1, in spite of
262 the higher CS, the particle formation rate at our site appears to be higher than those
263 in clean environments. This kind of intensive NPF becomes more noticeable for those
264 Chinese megacities, such as Shanghai, Beijing and Nanjing, having an even higher J and
265 CS compared to that at our GC site. The most plausible explanation could be the more
266 abundance of nucleating precursors for NPF in those polluted atmosphere, which is
267 clearly proved by the SA concentration, either measured or calculated. To be specific,
268 the mean SA concentration during NPF at our GC site was around $7 \cdot 10^6 \text{ cm}^{-3}$, a factor
269 of above 10-20 higher than that at Hyytiälä in Finland. The SA concentration during
270 NPF at Shanghai and Nanjing was even higher, being around $4 \cdot 10^7 \text{ cm}^{-3}$.

271

272

273

274

275

276



277 **Table 1.** Summaries of the parameters (average value) relevant for NPF event during wintertime in China
 278 and other countries.

Station	Period	Frequency	J ($\text{cm}^{-3}\cdot\text{s}^{-1}$)	GR ($\text{nm}\cdot\text{h}^{-1}$)	CS ($10^{-2}\cdot\text{s}^{-1}$)	SA ($10^6\cdot\text{cm}^{-3}$)	Reference
GC ^R	2018.11.18	-	3.15 (J_{10})	4.27	4.7	4.1	This study
GC ^R	2018.12.06	-	39.4 ($J_{1.34}$)	1.84	0.74	10.4	This study
GC ^R	2018.12.07	-	40.8 ($J_{1.34}$)	4.05	0.8	11.3	This study
GC ^R	2018.12.08	-	28.2 ($J_{1.34}$)	8.11	2.7	4.59	This study
GC ^R	2018.12.23	-	8.01 ($J_{1.34}$)	1.23	1.6	5.35	This study
GC ^R (mean)	2018.11.12-12.24	12.8%	29.1 ($J_{1.34}$)	3.9	2.1	7.15	This study
Thissio ^{UB}	2015.8-2016.8, 2017.2-2018.2 ^a	10.3%	1.55 (J_{10})	3.48	0.79	6.33	(Kalkavouras et al., 2020)
New Delhi ^U	2002.10.26-2002.11.9	53.3%	7.3 (J_3)	14.9	5.75	-	(Mönkkönen et al., 2005)
Panyu ^U	Winter of 2011	21.3%	0.89 (J_{10})	5.1	5.5	-	(Tan et al., 2016)
Shanghai ^U	2013.11.25-2014.1.25	21%	188 ($J_{1.34}$)	11.4	6.0	37	(Xiao et al., 2015)
Nanjing ^U	2011.11.18-2012.3.31	20%	33.2 (J_2)	8.5	2.4	45.3	(Herrmann et al., 2014)
Hongkong ^U	2010.10.25-2010.11.29	34.3%	2.94($J_{5.5}$)	3.86	0.8-6.2	9.17	(H. Guo et al., 2012)
Beijing ^U	2018.1.23-2018.3.31	51.5%	38 ($J_{1.5}$)	5.5	3.7	4.13	(Chu et al., 2021)
Ziyang ^R	2012.12.5-2013.1.5	23%	5.2(J_3)	3.6	7.4	6.7	(Chen et al., 2014)
Melpitz ^R	Winter of 2003-2006	3%	0.7 (J_3)	5.6	1.2	0.123	(Hamed et al., 2010)
Melpitz ^R	Winter of 1996-1997	10%	4.9(J_3)	4.1	0.9	0.259	(Hamed et al., 2010)
Pingyuan ^R	2017.11.3-2018.1.20	39.2%	164.2 ($J_{1.37}$)	3.9	1.9	2.45	(Fang et al., 2020)
Xinken ^R	2004.10.3-2004.11.5	25.9%	0.5-5.4(J_3)	2.2-19.8	-	-	(Liu et al., 2008)
Solapur ^R	2018.10-2019.2	28.9%	0.22-10.07(J_{15})	1.2-13.8	0.6-3	-	(Varghese et al., 2020)
Cyprus ^{RB}	2018.1-2018.2	69%	16.4($J_{1.5}$)	9.97	1.2	-	(Baalbaki et al., 2020)
SEAS ^O	Winter of 2018	5%	2.95(J_{10})	14.35	4.5	-	(Kompalli et al., 2020)
SMEAR II ^B	Winter of 1996-2003	24.2%	0.2-1.1(J_3)	0.29-3.7	0.05-0.35	0.53	(Dal Maso et al., 2005)



279 SEAS: the southeastern Arabian Sea
280 R: rural site UB: urban background site RB: rural background site U: urban site. B: background site O: ocean
281 site
282 a: only in wintertime -: no number



283 Although the formation rate of 1.34 nm particles is relatively high, the newly-formed
284 particles at our GC site usually cannot grow into very large particles within a short time,
285 indicative by their low GR. The average value of $GR_{1.34-2.4}$ and GR_{9-15} at our site was 0.54
286 nm/h and 3.9 nm/h, respectively, being generally lower than many clean environments
287 (GR_{1-3} of 0.9 nm/h for Hyytiälä, of 5.1 nm/h for Jungfrauoch), but similar to those at
288 urban Beijing and rural Pingyuan. This could be attributed by the high CS or CoagS at
289 those sites that small particles are vulnerable to the coagulation scavenging. However,
290 despite the high CoagS, the observed GR at Shanghai and Nanjing was still
291 exceptionally high. This discrepancy suggests that besides the high concentration of
292 precursors, mainly H_2SO_4 , in polluted environments including both rural and urban
293 sites, other precursors with different efficiency for nanoparticle growth, and other
294 involving mechanisms, for instance, multiphase reactions, may all contribute to the
295 nanoparticle growth, yet to be elucidated.

296 **3.2. Potential mechanisms for NPF events in the rural NCP**

297 To further understand the dominating nucleation mechanism in the rural atmosphere
298 of NCP in China, we plotted the measured formation rate of 1.34 nm particles ($J_{1.34}$)
299 against the simulated H_2SO_4 concentration and compared the results to previous
300 studies conducted in different environments, as shown in Fig. 4. The formation rate of
301 particles under similar H_2SO_4 level for our study approximated most to the formation
302 rates measured by these CLOUD (The Cosmics Leaving Outdoor Droplets chamber)
303 experiments using H_2SO_4 and DMA as the nucleating vapors. This suggested that
304 H_2SO_4 clustering drove the initial steps of NPF at our GC site, and the molecules
305 stabilizing H_2SO_4 clustering were most likely DMA.

306
307 For NPF in China, the $J_{1.34}$ - H_2SO_4 relationship in our results were also close to that in
308 Beijing (Cai et al., 2021), an urban site in the NCP, but with a lower formation rate
309 under similar H_2SO_4 level. Cai et al. (2021) and Yan et al. (2021) concluded that H_2SO_4 -
310 DMA was the dominating nucleation mechanism for urban Beijing with an additional



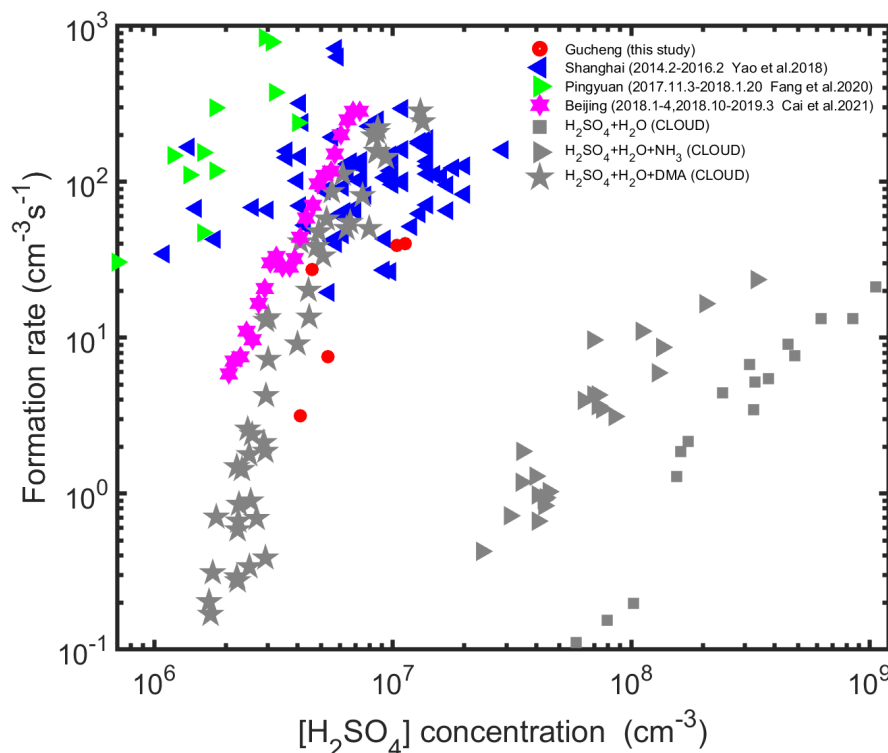
311 support from the measured C2-amine concentration. It has to be noted that their study
312 was conducted during a much longer time and completely covered the measurement
313 period of our study. More importantly, during the five days of events in our study, NPF
314 concurrently occurred at their measurement site (Liu et al., 2020). This suggests that
315 NPF events during these days in this region might be a regional phenomena, sharing
316 the same or similar nucleation mechanism. Therefore, we conclude that clustering of
317 H₂SO₄ with DMA may also dominate the nucleation process at our site during winter.
318

319 On the other hand, we noticed that our results deviates significantly from the
320 measured formation rate at Pingyuan (Fang et al., 2020), another rural site in the NCP.
321 They concluded that neither H₂SO₄-NH₃ nor H₂SO₄-DMA mechanisms could fully
322 explain their observed particle formation rate but suggested that gaseous dicarboxylic
323 acids were the dominating species for the initial step of H₂SO₄ clustering under diacid-
324 rich environment. Being likewise the rural environment of NCP, we cannot completely
325 rule out the contribution of dicarboxylic acids to the H₂SO₄ stabilizing. However, by
326 taking into account the contribution from dicarboxylic acid (measured by a iodine-
327 based chemical ionization-atmospheric pressure interface-time-of-flight (I-API-TOF,
328 Aerodyne Research Inc., USA)), the obtained J_{1,34}-H₂SO₄×diacids relationship was not
329 improved (see Fig. S1), being obviously different from the case of Pingyuan. Hence, the
330 involvements of diacids during the initial steps of nucleation under current rural
331 atmosphere cannot be confirmed, requiring future data, for instance, the signal of
332 H₂SO₄-diacids to be elucidated. This statement does not necessarily mean that our
333 previous inference was incorrect, but on the other side, provides some hints that
334 though NPF events in the NCP is regional, there might be no uniform theory but
335 multiple mechanisms coexisting to explain its feature with the dominating one varies
336 upon different emission patterns or meteorological conditions.

337

338

339



340
341 **Figure 4.** The particle formation rate ($J_{1,34}$) as a function of H_2SO_4 concentration for our study as
342 well as for urban Shanghai, Beijing, rural Pingyuan and CLOUD measurements. Gray square,
343 triangle, pentagram, and diamond represents the CLOUD data for $\text{H}_2\text{SO}_4+\text{H}_2\text{O}$, $\text{H}_2\text{SO}_4+\text{H}_2\text{O}+\text{NH}_3$,
344 $\text{H}_2\text{SO}_4+\text{H}_2\text{O}+\text{DMA}$ (Kirkby et al. (2011) and Riccobono et al. (2014)), where DMA represents
345 dimethylamine.

346

347 **3.3 Governing factors for the occurrence of NPF in rural NCP**

348

349 The high concentration of SO_2 , NH_3 , NO_x , VOCs as well as fine particles makes the NCP
350 of China an unique condition for NPF compared to many other environments. In
351 principle, the competition between how fast the newly-formed clusters grow and how
352 fast they are scavenged determines whether NPF will occur or not in the atmosphere.
353 However, in the NCP, the concentration of SA was typically quite high, probably
354 reaching its maximum rate to form clusters. Thus, CS or CoagS becomes the dominant
355 factor controlling the occurrence of NPF. This was partly confirmed by existing



356 observations, for instance, Cai et al. (2021) found that H₂SO₄ was high enough in
357 urban Beijing, but not necessarily led to the occurrence of NPF there. They pointed out
358 that as long as CS or CoagS was below a certain threshold (Cai et al., 2017), NPF is very
359 likely take place.

360

361 Was this also true for rural atmosphere in the NCP? By comparing with event days at
362 our site, we noticed that CS level was in general higher during non-event days. In other
363 words, NPF was very likely to occur when CS was significantly lowered. This strongly
364 demonstrates the similarity between our site with urban Beijing, that CS would be the
365 limiting factor for the occurrence of NPF. However, we noticed that besides the higher
366 CS, the H₂SO₄ concentration was also in general lower during non-event days
367 compared to event days. Particularly, there were a very few cases that CS was
368 somewhat quite low (<0.06 /s), being quite close to that under those event days, yet
369 NPF still did not occur, most likely owing to the lowered H₂SO₄ concentration at these
370 days. This implies that nucleating species, such as H₂SO₄, may not be always enough
371 to initiate nucleation at this site compared to urban Beijing, where pollution level were
372 typically higher. Under a certain CS, the level of H₂SO₄ relies on both the solar
373 radiation reaching to the Earth's surface and the concentration of gaseous SO₂. By
374 looking at both content during non-event days (Fig. S2), we found that the
375 concentration of SO₂ was comparable to that at Beijing and even far beyond that in
376 many clean environments that needed to initiate nucleation (for example, around 1
377 ppb in Hyytiälä). This means that the reduced solar radiation intensity was the main
378 reason determining the lower level of H₂SO₄ and thus controlling atmospheric NPF
379 not occur.

380

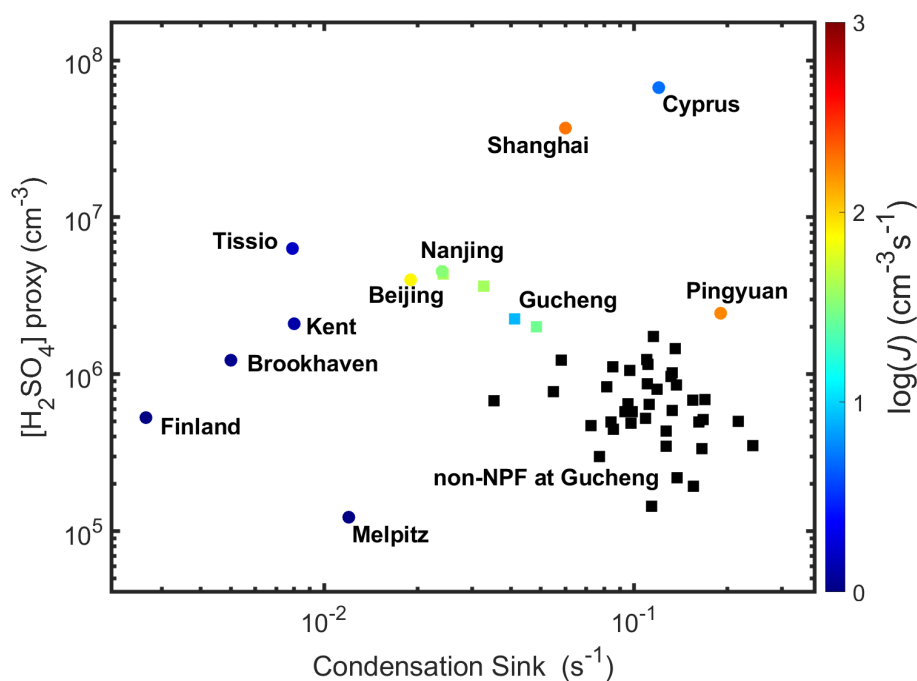
381 Taking both, we conclude that CS or CoagS was the dominating factor that governing
382 the occurrence and intensity of NPF at our GC site, while the influence from the
383 available H₂SO₄ is not negligible, either. The available H₂SO₄ was found to be mainly
384 determined by the solar radiation intensity reaching to the Earth but not SO₂ level in
385 the atmosphere. This would be a general characteristic of NPF events in this region



386 compared to urban atmosphere of China, where threshold for CS was solely needed
387 for the appearance of NPF. Nevertheless, this pattern is also different from other
388 western countries, where the intensity of nucleating or condensable species is the
389 limiting and perhaps the only factor for the occurrence of NPF (Wang et al., 2017;
390 Kulmama et al., 2016; Kerminen et al., 2018).

391

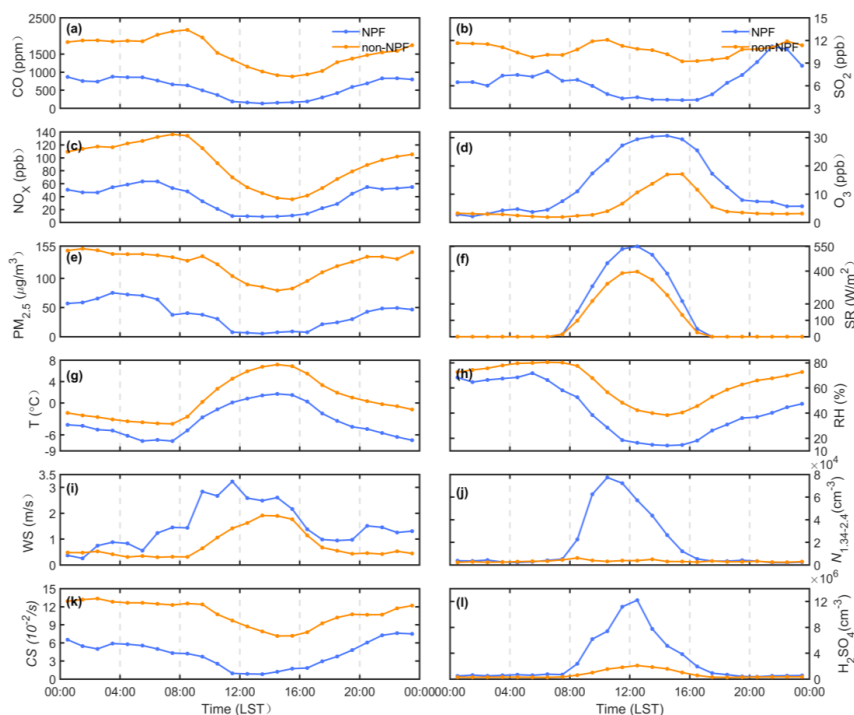
392



393

394 **Figure 5.** Condensation sink and H_2SO_4 concentration in various atmospheric environments,
395 including Finland (Nieminen et al., 2014), TISSIO (Kalkavouras et al., 2020), Cyprus (Baalbaki et al.,
396 2020), Melpitz (Hamed et al., 2010), Brookhaven (Yu et al., 2014), Kent (Yu et al., 2014), Pingyuan
397 (Fang et al., 2020), Beijing (Deng et al., 2020), Nanjing (Herrmann et al., 2014), and Shanghai (Yao
398 et al., 2018) site. The color bar indicates particle formation rate.

399



400
401 **Figure 6.** Diurnal variation of (a) CO, (b) SO₂, (c) NO_x, (d) O₃, (e) PM_{2.5}, (f) Solar radiation (SR), (g) *T*,
402 (h) RH, (i) wind speed (WS), (j) number concentration of sub-3nm cluster, (k) CS, and (l) H₂SO₄ proxy
403 during the NPF and non-NPF days during this field campaign.

404
405 On the other hand, we found that RH level under event days was generally lower than
406 that on non-event days (see Fig. 6). This is similar to the cases that NPF was observed
407 in Beijing by Yue et al. (2009), who suggested that photochemical reactions were faster
408 on sunny days with low RH. In addition to this, ambient temperature during NPF was
409 relatively lower than that on non-event days. Yan et al. (2021) considered that
410 temperature can affect the stability of H₂SO₄ clustering and thus influence NPF.
411 Therefore, all these factors could be the potential reasons increase or decrease the
412 probability of NPF to occur in current rural areas. It has to be noted that all these
413 features, including reduced RH level as well as ambient *T* during event days, could be
414 coincidence with reduced CS over clean days, for instance, being a consequence of air
415 masses originating from the north and bringing dryer, colder and cleaner air to the site.



416 Therefore, current discussion in this regard becomes ambiguous and may be inclusive,
417 but should still be considered separately when larger datasets are available. Moreover,
418 we observed that O₃ concentration was clearly higher during event days, implying that
419 other condensable vapours, for instance, organics, that involving O₃ oxidation, might
420 also be important to NPF in this region. Although these oxygenated organic
421 compounds may not necessarily participate in H₂SO₄ clustering, they may
422 considerably contribute to the growth of newly-formed particles, which should not be
423 ruled out in the study of NPF for this region and also need to be investigated in the
424 future.

425

426 4. Summary and conclusions

427

428 Most previous studies dealing with NPF in China were mainly based on measurements
429 of particles at larger sizes, typically above 3 nm, whereas detection of particles at sub-
430 3 nm range was quite limited. In our study, by coupling a PSM with a traditional SMPS,
431 We were able to measure the particle number size distribution down to 1.34 nm during
432 NPF events in the wintertime at a rural site of the NCP. Correspondingly, formation rate
433 of particles at 1.34 nm was obtained, widening the data pool concerning the feature
434 of NPF for this region. At current rural environment, high level of H₂SO₄ or low
435 concentration of fine particles may not always initiate the occurrence of NPF. Only at
436 the condition that the concentration of H₂SO₄ was relatively high and CS was
437 considerably low, NPF events were more likely to take place. This feature is slightly
438 different from that of the urban atmosphere of NCP, whereas NPF events were usually
439 characterized with high formation rate, high CS and high H₂SO₄ concentration.
440 However, as our H₂SO₄ concentration was predicted from empirical parameters,
441 particular cautions regarding their associated uncertainties should be considered. At
442 urban Beijing, NPF was also observed during the wintertime of 2018. We found that
443 their measured H₂SO₄ concentration was quite comparable to the predicted ones in
444 our study, indicating its relative reliability in using them though absolute uncertainties
445 could not be derived here. Yang et al. (2021) demonstrated that the derived fitting



446 parameters for the calculations of H_2SO_4 proxy may vary from site to site and between
447 different seasons. For instance, they considered the products from the ozonolysis of
448 alkenes were able to oxidize SO_2 to form gaseous H_2SO_4 . Moreover, they pointed out
449 that H_2SO_4 could be from primary emissions, such as vehicles, or freshly emitted
450 plumes, which could account for 10% of the total H_2SO_4 in the atmosphere. These
451 aspects were not comprehensively considered in our calculations, which could bring
452 huge uncertainties or errors to the estimation. Thereby, though the H_2SO_4 proxy was
453 approximated to the measured ones at Beijing site, direct measurements for the H_2SO_4
454 concentration should be implemented in the future before driving any further
455 conclusion.

456

457

458

459

460

461

462

463

464

465

466

467

468

469

470

471

472

473

474

475



476 **Declaration of interest statement.**

477 The authors declare that they have no known competing financial interests or personal
478 relationships that could have appeared to influence the work reported in this paper.

479

480 **Data availability.**

481 The details data can be obtained from <https://doi.org/10.5281/zenodo.7326388>
482 (Hong, 2022).

483

484 **Author contributions.**

485 JH collected the resources, wrote and finalized the manuscript, MT analyzed the data,
486 plotted the figures and wrote the original draft, QQW and NM planned the study,
487 collected the resources, reviewed the manuscript. SWZ, SBZ, XHP, LHX, GL, UK
488 conducted the measurements, CY, JCT, YK, YH, YQZ, WYX, GSZ, BY, ZBW discussed the
489 results. YFC and HS contributed to fund acquisition.

490

491 **Competing interests.**

492 Hang Su and Yafang Cheng are members of the editorial board of Atmospheric
493 Chemistry and Physics

494

495 **Acknowledgements.**

496 This work is supported by the National Natural Science Foundation of China (grant no.
497 42175117, 41907182, 41877303, 91644218) and the National key R&D Program of
498 China (2018YFC0213901), the Fundamental Research Funds for the Central
499 Universities (21621105), the Guangdong Innovative and Entrepreneurial Research
500 Team Program (Research team on atmospheric environmental roles and effects of
501 carbonaceous species: 2016ZT06N263), and Special Fund Project for Science and
502 Technology Innovation Strategy of Guangdong Province (2019B121205004).



503 References

- 504 Almeida, J., Schobesberger, S., Kürten, A., Ortega, I. K., Kupiainen-Määttä, O., Praplan, A. P., Adamov,
505 A., Amorim, A., Bianchi, F., Breitenlechner, M., David, A., Dommen, J., Donahue, N. M.,
506 Downard, A., Dunne, E., Duplissy, J., Ehrhart, S., Flagan, R. C., Franchin, A., ... Kirkby, J. (2013).
507 Molecular understanding of sulphuric acid-amine particle nucleation in the atmosphere. *Nature*,
508 502(7471), 359–363. <https://doi.org/10.1038/nature12663>
- 509 Baalbaki, R., Pikridas, M., Jokinen, T., Laurila, T., Dada, L., Bezantakos, S., Ahonen, L., Neitola, K.,
510 Maisser, A., Bimenyimana, E., Christodoulou, A., Unga, F., Savvides, C., Lehtipalo, K.,
511 Kangasluoma, J., Biskos, G., Petäjä, T., Kerminen, V.-M., Sciare, J., & Kulmala, M. (2020).
512 Towards understanding the mechanisms of new particle formation in the Eastern
513 Mediterranean. *Atmospheric Chemistry and Physics Discussions*, November, 1–44.
514 <https://doi.org/10.5194/acp-2020-1066>
- 515 Berndt, T., Stratmann, F., Sipilä, M., Vanhanen, J., Petäjä, T., Mikkilä, J., Grüner, A., Spindler, G., Lee
516 Mauldin, R., Curtius, J., Kulmala, M., & Heintzenberg, J. (2010). Laboratory study on new particle
517 formation from the reaction OH + SO₂: Influence of experimental conditions, H₂O vapour, NH₃
518 and the amine tert-butylamine on the overall process. *Atmospheric Chemistry and Physics*,
519 10(15), 7101–7116. <https://doi.org/10.5194/acp-10-7101-2010>
- 520 Bianchi, F., Tröstl, J., Junninen, H., Frege, C., Henne, S., Hoyle, C. R., Molteni, U., Herrmann, E.,
521 Adamov, A., Bukowiecki, N., Chen, X., Duplissy, J., Gysel, M., Hutterli, M., Kangasluoma, J.,
522 Kontkanen, J., Kürten, A., Manninen, H. E., Münch, S., ... Baltensperger, U. (2016). New particle
523 formation in the free troposphere: A question of chemistry and timing. *Science*, 352(6289),
524 1109–1112. <https://doi.org/10.1126/science.aad5456>
- 525 Cai, R., & Jiang, J. (2017). A new balance formula to estimate new particle formation rate:
526 Reevaluating the effect of coagulation scavenging. *Atmospheric Chemistry and Physics*, 17(20),
527 12659–12675. <https://doi.org/10.5194/acp-17-12659-2017>
- 528 Cai, R., Yan, C., Yang, D., Yin, R., Lu, Y., Deng, C., Fu, Y., Ruan, J., Li, X., Kontkanen, J., Zhang, Q.,
529 Kangasluoma, J., Ma, Y., Hao, J., Worsnop, D. R., Bianchi, F., Paasonen, P., Kerminen, V. M., Liu,
530 Y., ... Jiang, J. (2021). Sulfuric acid-amine nucleation in urban Beijing. *Atmospheric Chemistry and*
531 *Physics*, 21(4), 2457–2468. <https://doi.org/10.5194/acp-21-2457-2021>
- 532 CHEN Chen, HU Min, WU Zhi-jun, WU Yu-sheng, GUO Song, CHEN Wen-tai, LUO Bin, SHAO Min,
533 ZHANG Yuan-hang, X. S. (2014). Characterization of new particle formation event in the rural
534 site of Sichuan Basin and its contribution to cloud condensation nuclei. *China Environmental*
535 *Science*, 34(11), 2764–2772.
- 536 Chu, B., Dada, L., Liu, Y., Yao, L., Wang, Y., Du, W., Cai, J., Dällenbach, K. R., Chen, X., Simonen, P.,
537 Zhou, Y., Deng, C., Fu, Y., Yin, R., Li, H., He, X. C., Feng, Z., Yan, C., Kangasluoma, J., ... Kulmala, M.
538 (2021). Particle growth with photochemical age from new particle formation to haze in the
539 winter of Beijing, China. *Science of the Total Environment*, 753, 142207.
540 <https://doi.org/10.1016/j.scitotenv.2020.142207>
- 541 Chu, B., Veli-Matti Kerminen, Federico Bianchi, Chao Yan, Tuukka Petäjä, & Markku Kulmala. (2019).
542 Atmospheric new particle formation in China. *Atmospheric Chemistry and Physics*, 115–138.
- 543 Dal Maso, M., Kulmala, M., Riipinen, I., Wagner, R., Hussein, T., Aalto, P. P., & Lehtinen, K. E. J. (2005).
544 Formation and growth of fresh atmospheric aerosols: Eight years of aerosol size distribution



- 545 data from SMEAR II, Hyytiälä, Finland. *Boreal Environment Research*, 10(5), 323–336.
- 546 Deng, C., Fu, Y., Dada, L., Yan, C., Cai, R., Yang, D., Zhou, Y., Yin, R., Lu, Y., Li, X., Qiao, X., Fan, X., Nie,
547 W., Kontkanen, J., Kangasluoma, J., Chu, B., Ding, A., Kerminen, V.-M., Paasonen, P., ... Jiang, J.
548 (2020). Seasonal Characteristics of New Particle Formation and Growth in Urban Beijing.
549 *Environmental Science & Technology*, acs.est.0c00808. <https://doi.org/10.1021/acs.est.0c00808>
- 550 Dunne, E. M., Gordon, H., Kürten, A., Almeida, J., Duplissy, J., Williamson, C., Ortega, I. K., Pringle, K. J.,
551 Adamov, A., Baltensperger, U., Barmet, P., Benduhn, F., Bianchi, F., Breitenlechner, M., Clarke,
552 A., Curtius, J., Dommen, J., Donahue, N. M., Ehrhart, S., ... Carslaw, K. S. (2016). Global
553 atmospheric particle formation from CERN CLOUD measurements. *Science*, 354(6316), 1119–
554 1124. <https://doi.org/10.1126/science.aaf2649>
- 555 Ehn, M., Thornton, J. A., Kleist, E., Sipilä, M., Junninen, H., Pullinen, I., Springer, M., Rubach, F.,
556 Tillmann, R., Lee, B., Lopez-Hilfiker, F., Andres, S., Acir, I.-H., Rissanen, M., Jokinen, T.,
557 Schobesberger, S., Kangasluoma, J., Kontkanen, J., Nieminen, T., ... Mentel, T. F. (2014). A large
558 source of low-volatility secondary organic aerosol. *Nature*, 506(7489), 476–479.
559 <https://doi.org/10.1038/nature13032>
- 560 Fang, X., Hu, M., Shang, D., Tang, R., Shi, L., Olenius, T., Wang, Y., Wang, H., Zhang, Z., Chen, S., Yu, X.,
561 Zhu, W., Lou, S., Ma, Y., Li, X., Zeng, L., Wu, Z., Zheng, J., & Guo, S. (2020). Observational
562 Evidence for the Involvement of Dicarboxylic Acids in Particle Nucleation. *Environmental Science
563 & Technology Letters*. <https://doi.org/10.1021/acs.estlett.0c00270>
- 564 Guo, H., Wang, D. W., Cheung, K., Ling, Z. H., Chan, C. K., & Yao, X. H. (2012). Observation of aerosol
565 size distribution and new particle formation at a mountain site in subtropical Hong Kong.
566 *Atmospheric Chemistry and Physics*, 12(20), 9923–9939. [https://doi.org/10.5194/acp-12-9923-
567 2012](https://doi.org/10.5194/acp-12-9923-2012)
- 568 Guo, S., Hu, M., Zamora, M. L., Peng, J., Shang, D., Zheng, J., Du, Z., Wu, Z., Shao, M., Zeng, L., Molina,
569 M. J., & Zhang, R. (2014). Elucidating severe urban haze formation in China. *Proceedings of the
570 National Academy of Sciences of the United States of America*, 111(49), 17373–17378.
571 <https://doi.org/10.1073/pnas.1419604111>
- 572 Hamed, A., Birmili, W., Joutsensaari, J., Mikkonen, S., Asmi, A., Wehner, B., Spindler, G., Jaatinen, A.,
573 Wiedensohler, A., Korhonen, H., J. Lehtinen, K. E., & Laaksonen, A. (2010). Changes in the
574 production rate of secondary aerosol particles in Central Europe in view of decreasing SO₂
575 emissions between 1996 and 2006. *Atmospheric Chemistry and Physics*, 10(3), 1071–1091.
576 <https://doi.org/10.5194/acp-10-1071-2010>
- 577 Herrmann, E., Ding, A. J., Kerminen, V. M., Petäjä, T., Yang, X. Q., Sun, J. N., Qi, X. M., Manninen, H.,
578 Hakala, J., Nieminen, T., Aalto, P. P., Kulmala, M., & Fu, C. B. (2014). Aerosols and nucleation in
579 eastern China: First insights from the new SORPES-NJU station. *Atmospheric Chemistry and
580 Physics*, 14(4), 2169–2183. <https://doi.org/10.5194/acp-14-2169-2014>
- 581 Hong J.: Data for “intertime new particle formation in the rural area of North China Plain:
582 influencing factors and possible formation mechanism”, Zenodo [data set],
583 <https://doi.org/10.5281/zenodo.7326388>.
- 584 Hussein, T., Dal Maso, M., Petäjä, T., Koponen, I. K., Paatero, P., Aalto, P. P., Hämeri, K., & Kulmala, M.
585 (2005). Evaluation of an automatic algorithm for fitting the particle number size distributions.
586 *Boreal Environment Research*, 10(5), 337–355.
- 587 Kalkavouras, P., Bougiatioti, A., Grivas, G., Stavroulas, I., Kalivitis, N., Liakakou, E., Gerasopoulos, E.,
588 Pilinis, C., & Mihalopoulos, N. (2020). On the regional aspects of new particle formation in the



- 589 Eastern Mediterranean: A comparative study between a background and an urban site based on
590 long term observations. *Atmospheric Research*, 239(January), 104911.
591 <https://doi.org/10.1016/j.atmosres.2020.104911>
- 592 Kangasluoma, J., Franchin, A., Duplissy, J., Ahonen, L., Korhonen, F., Attoui, M., Mikkilä, J., Lehtipalo,
593 K., Vanhanen, J., Kulmala, M., & Petäjä, T. (2016). Operation of the Airmodus A11 nano
594 Condensation Nucleus Counter at various inlet pressures and various operation temperatures,
595 and design of a new inlet system. *Atmospheric Measurement Techniques*, 9(7), 2977–2988.
596 <https://doi.org/10.5194/amt-9-2977-2016>
- 597 Kerminen, V. M., Chen, X., Vakkari, V., Petäjä, T., Kulmala, M., & Bianchi, F. (2018). Atmospheric new
598 particle formation and growth: Review of field observations. In *Environmental Research Letters*
599 (Vol. 13, Issue 10, p. 103003). <https://doi.org/10.1088/1748-9326/aadf3c>
- 600 Kirkby, J., Curtius, J., Almeida, J., Dunne, E., Duplissy, J., Ehrhart, S., Franchin, A., Gagné, S., Ickes, L.,
601 Kürten, A., Kupc, A., Metzger, A., Riccobono, F., Rondo, L., Schobesberger, S., Tsagkogeorgas, G.,
602 Wimmer, D., Amorim, A., Bianchi, F., ... Kulmala, M. (2011). Role of sulphuric acid, ammonia and
603 galactic cosmic rays in atmospheric aerosol nucleation. *Nature*, 476(7361), 429–435.
604 <https://doi.org/10.1038/nature10343>
- 605 Kirkby, J., Duplissy, J., Sengupta, K., Frege, C., Gordon, H., Williamson, C., Heinritzi, M., Simon, M., Yan,
606 C., Almeida, J., Trostl, J., Nieminen, T., Ortega, I. K., Wagner, R., Adamov, A., Amorim, A.,
607 Bernhammer, A. K., Bianchi, F., Breitenlechner, M., ... Curtius, J. (2016). Ion-induced nucleation
608 of pure biogenic particles. *Nature*, 533(7604), 521–526. <https://doi.org/10.1038/nature17953>
- 609 Kompalli, S. K., Nair, V. S., Jayachandran, V., Gogoi, M. M., & Babu, S. S. (2020). Particle number size
610 distributions and new particle formation events over the northern Indian Ocean during
611 continental outflow. *Atmospheric Environment*, 238(April), 117719.
612 <https://doi.org/10.1016/j.atmosenv.2020.117719>
- 613 Kulmala, M. (2013). Direct Observations of Atmospheric Aerosol Nucleation. *Science*, 943.
614 <https://doi.org/10.1126/science.1227385>
- 615 Kulmala, M., Petäjä, T., Ehn, M., Thornton, J., Sipilä, M., Worsnop, D. R., & Kerminen, V. M. (2014).
616 Chemistry of atmospheric nucleation: On the recent advances on precursor characterization and
617 atmospheric cluster composition in connection with atmospheric new particle formation.
618 *Annual Review of Physical Chemistry*, 65, 21–37. <https://doi.org/10.1146/annurev-physchem-040412-110014>
- 620 Kulmala, M., Petäjä, T., Nieminen, T., Sipilä, M., Manninen, H. E., Lehtipalo, K., Maso, M. D., Aalto, P.
621 P., Junninen, H., Paasonen, P., Riipinen, I., Lehtinen, K. E. J., Laaksonen, A., & Kerminen, V.
622 (2012). Measurement of the nucleation of atmospheric aerosol particles. *Nature Protocols*, 7(9),
623 1651–1667. <https://doi.org/10.1038/nprot.2012.091>
- 624 Kulmala, M., Pirjola, L., & Mäkelä, J. M. (2000). Stable sulphate clusters as a source of new
625 atmospheric particles. *Nature*, 404(6773), 66–69. <https://doi.org/10.1038/35003550>
- 626 Kulmala, M., Vehkamäki, H., Petäjä, T., Dal Maso, M., Lauri, A., Kerminen, V. M., Birmili, W., &
627 McMurry, P. H. (2004). Formation and growth rates of ultrafine atmospheric particles: A review
628 of observations. *Journal of Aerosol Science*, 35(2), 143–176.
629 <https://doi.org/10.1016/j.jaerosci.2003.10.003>
- 630 Kulmala, M., Petäjä, T., Kerminen, V. M., Kujansuu, J., Ruuskanen, T., Ding, A., Nie, W., Hu, M., Wang,
631 Z., Wu, Z., Wang, L., & Worsnop, D. R. (2016). On secondary new particle formation in China.
632 *Frontiers of Environmental Science and Engineering*, 10(5), 1–10.



- 633 <https://doi.org/10.1007/s11783-016-0850-1>
- 634 Kürten, A., Bergen, A., Heinritzi, M., Leiminger, M., Lorenz, V., Piel, F., Simon, M., Sitals, R., Wagner, A.
635 C., & Curtius, J. (2016). Observation of new particle formation and measurement of sulfuric acid,
636 ammonia, amines and highly oxidized organic molecules at a rural site in central Germany.
637 *Atmospheric Chemistry and Physics*, 16(19), 12793–12813. [https://doi.org/10.5194/acp-16-](https://doi.org/10.5194/acp-16-12793-2016)
638 [12793-2016](https://doi.org/10.5194/acp-16-12793-2016)
- 639 Lin, W., Xu, X., Ge, B., & Zhang, X. (2009). Characteristics of gaseous pollutants at Gucheng, a rural site
640 southwest of Beijing. *Journal of Geophysical Research Atmospheres*, 114(16).
641 <https://doi.org/10.1029/2008JD010339>
- 642 Liu, S., Hu, M., Wu, Z., Wehner, B., Wiedensohler, A., & Cheng, Y. (2008). Aerosol number size
643 distribution and new particle formation at a rural/coastal site in Pearl River Delta (PRD) of
644 China. *Atmospheric Environment*, 42(25), 6275–6283.
645 <https://doi.org/10.1016/j.atmosenv.2008.01.063>
- 646 Liu, Y., Yan, C., Feng, Z., Zheng, F., Fan, X., Zhang, Y., Li, C., Zhou, Y., Lin, Z., Guo, Y., Zhang, Y., Ma, L.,
647 Zhou, W., Liu, Z., Dada, L., Dällenbach, K., Kontkanen, J., Cai, R., Chan, T., ... Kulmala, M. (2020).
648 Continuous and comprehensive atmospheric observations in Beijing: a station to understand
649 the complex urban atmospheric environment. *Big Earth Data*, 4(3), 295–321.
650 <https://doi.org/10.1080/20964471.2020.1798707>
- 651 Ma, N., Zhao, C., Tao, J., Wu, Z., Kecorius, S., Wang, Z., Groß, J., Liu, H., Bian, Y., Kuang, Y., Teich, M.,
652 Spindler, G., Müller, K., Van Pinxteren, D., Herrmann, H., Hu, M., & Wiedensohler, A. (2016).
653 Variation of CCN activity during new particle formation events in the North China Plain.
654 *Atmospheric Chemistry and Physics*, 16(13), 8593–8607. [https://doi.org/10.5194/acp-16-8593-](https://doi.org/10.5194/acp-16-8593-2016)
655 [2016](https://doi.org/10.5194/acp-16-8593-2016)
- 656 Mikko Sipilä, Torsten Berndt, Tuukka Petäjä, David Brus, Joonas Vanhanen, Frank Stratmann, Johanna
657 Patokoski, Roy L. Mauldin III, Antti-Pekka Hyvärinen, Frank Stratmann, Johanna Patokoski, Roy L.
658 Mauldin III, Heikki Lihavainen, M. K. (2010). The Role of Sulfuric Acid in Atmospheric Nucleation.
659 *Science*, 327(MARCH), 1243–1246.
- 660 Mönkkönen, P., Koponen, I. K., Lehtinen, K. E. J., Hämeri, K., Uma, R., & Kulmala, M. (2005).
661 Measurements in a highly polluted Asian mega city: observations of aerosol number size
662 distribution, modal parameters and nucleation events. *Atmospheric Chemistry and Physics*
663 *Discussions*, 4(5), 5407–5431. <https://doi.org/10.5194/acpd-4-5407-2004>
- 664 Nieminen, T., Asmi, A., Aalto, P. P., Keronen, P., Petäjä, T., Kulmala, M., Kerminen, V. M., Nieminen, T.,
665 & Dal Maso, M. (2014). Trends in atmospheric new-particle formation: 16 years of observations
666 in a boreal-forest environment. *Boreal Environment Research*, 19(September), 191–214.
- 667 Nieminen, T., Lehtinen, K. E. J., & Kulmala, M. (2010). Sub-10 nm particle growth by vapor
668 condensation-effects of vapor molecule size and particle thermal speed. *Atmospheric Chemistry*
669 *and Physics*, 10(20), 9773–9779. <https://doi.org/10.5194/acp-10-9773-2010>
- 670 Petäjä, T., Mauldin, R. L., Kosciuch, E., McGrath, J., Nieminen, T., Paasonen, P., Boy, M., Adamov, A.,
671 Kotiaho, T., & Kulmala, M. (2009). Sulfuric acid and OH concentrations in a boreal forest site.
672 *Atmospheric Chemistry and Physics*, 9(19), 7435–7448. [https://doi.org/10.5194/acp-9-7435-](https://doi.org/10.5194/acp-9-7435-2009)
673 [2009](https://doi.org/10.5194/acp-9-7435-2009)
- 674 Petzold, A., Ogren, J. A., Fiebig, M., Laj, P., Li, S. M., Baltensperger, U., Holzer-Popp, T., Kinne, S.,
675 Pappalardo, G., Sugimoto, N., Wehrli, C., Wiedensohler, A., & Zhang, X. Y. (2013).
676 Recommendations for reporting black carbon measurements. *Atmospheric Chemistry and*



- 677 *Physics*, 13(16), 8365–8379. <https://doi.org/10.5194/acp-13-8365-2013>
- 678 Pushpawela, B., Jayaratne, R., & Morawska, L. (2019). The influence of wind speed on new particle
679 formation events in an urban environment. *Atmospheric Research*, 215(April 2018), 37–41.
680 <https://doi.org/10.1016/j.atmosres.2018.08.023>
- 681 Riccobono, F., Schobesberger, S., Scott, C. E., Dommen, J., Ortega, I. K., Rondo, L., Almeida, J.,
682 Amorim, A., Bianchi, F., Breitenlechner, M., David, A., Downard, A., Dunne, E. M., Duplissy, J.,
683 Ehrhart, S., Flagan, R. C., Franchin, A., Hansel, A., Junninen, H., ... Baltensperger, U. (2014).
684 Oxidation products of biogenic emissions contribute to nucleation of atmospheric particles.
685 *Science*, 344(6185), 717–721. <https://doi.org/10.1126/science.1243527>
- 686 Shen, X., Sun, J., Kivekäs, N., Kristensson, A., Zhang, X., Zhang, Y., Zhang, L., Fan, R., Qi, X., Ma, Q., &
687 Zhou, H. (2018). Spatial distribution and occurrence probability of regional new particle
688 formation events in eastern China. *Atmospheric Chemistry and Physics*, 18(2), 587–599.
689 <https://doi.org/10.5194/acp-18-587-2018>
- 690 Shen, X., Sun, J., Zhang, X., Zhang, Y., Wang, Y., Tan, K., Wang, P., Zhang, L., Qi, X., Che, H., Zhang, Z.,
691 Zhong, J., Zhao, H., & Ren, S. (2018). Comparison of Submicron Particles at a Rural and an Urban
692 Site in the North China Plain during the December 2016 Heavy Pollution Episodes. *Journal of*
693 *Meteorological Research*, 32(1), 26–37. <https://doi.org/10.1007/s13351-018-7060-7>
- 694 Spracklen, D. V., Carslaw, K. S., Kulmala, M., Kerminen, V. M., Mann, G. W., & Sihto, S. L. (2006). The
695 contribution of boundary layer nucleation events to total particle concentrations on regional
696 and global scales. *Atmospheric Chemistry and Physics*, 6(12), 5631–5648.
697 <https://doi.org/10.5194/acp-6-5631-2006>
- 698 Stolzenburg, D., Simon, M., Ranjithkumar, A., Kürten, A., Lehtipalo, K., Gordon, H., Ehrhart, S.,
699 Finkenzeller, H., Pichelstorfer, L., Nieminen, T., He, X., Brilke, S., Xiao, M., Amorim, A., Baalbaki,
700 R., Baccarini, A., & Beck, L. (2020). Enhanced growth rate of atmospheric particles from sulfuric
701 acid. *Atmospheric Chemistry and Physics*, November 2019, 7359–7372.
- 702 Sulo, J., Sarnela, N., Kontkanen, J., Ahonen, L., Paasonen, P., & Laurila, T. (2020). Long-term
703 measurement of sub-3nm particles and their precursor gases in the boreal forest. *Atmospheric*
704 *Chemistry and Physics*, July, 1–38.
- 705 Sun, Y., Wang, Z., Dong, H., Yang, T., Li, J., Pan, X., Chen, P., & Jayne, J. T. (2012). Characterization of
706 summer organic and inorganic aerosols in Beijing, China with an Aerosol Chemical Speciation
707 Monitor. *Atmospheric Environment*, 51, 250–259.
708 <https://doi.org/10.1016/j.atmosenv.2012.01.013>
- 709 Tan, H. B., Yin, Y., Li, F., Liu, X. T., Chan, P. W., Deng, T., Deng, X. J., Wan, Q. L., & Wu, D. (2016).
710 Measurements of particle number size distributions and new particle formation events during
711 winter in the Pearl River Delta region, China. *Journal of Tropical Meteorology*, 22(2), 191–199.
712 <https://doi.org/10.16555/j.1006-8775.2016.02.009>
- 713 Tröstl, J., Chuang, W. K., Gordon, H., Heinritzi, M., Yan, C., Molteni, U., Ahlm, L., Frege, C., Bianchi, F.,
714 Wagner, R., Simon, M., Lehtipalo, K., Williamson, C., Craven, J. S., Duplissy, J., Adamov, A.,
715 Almeida, J., Bernhammer, A. K., Breitenlechner, M., ... Baltensperger, U. (2016). The role of low-
716 volatility organic compounds in initial particle growth in the atmosphere. *Nature*, 533(7604),
717 527–531. <https://doi.org/10.1038/nature18271>
- 718 Vanhanen, J., Mikkilä, J., Lehtipalo, K., Sipil, M., Manninen, H. E., Siivola, E., & Pet, T. (2011). Particle
719 Size Magnifier for Nano-CN Detection. *Aerosol Science and Technology*, 533–542.
720 <https://doi.org/10.1080/02786826.2010.547889>



- 721 Varghese, M., Leena, P. P., Murugavel, P., Bankar, S., Todekar, K., Chowdhuri, S., Safai, P. D., Malap,
722 N., Konwar, M., Dixit, S., Rao, Y. J., & Prabha, T. V. (2020). New Particle Formation Observed
723 from a Rain Shadow Region of the Western Ghats India. *Toxicological and Environmental*
724 *Chemistry*, 0(0), 1–29. <https://doi.org/10.1080/02772248.2020.1789134>
- 725 Wang, Y., Kangasluoma, J., Attoui, M., Fang, J., Junninen, H., Kulmala, M., Petäjä, T., & Biswas, P.
726 (2017). The high charge fraction of flame-generated particles in the size range below 3 nm
727 measured by enhanced particle detectors. *Combustion and Flame*, 176, 72–80.
728 <https://doi.org/10.1016/j.combustflame.2016.10.003>
- 729 Wang, Z. B., Hu, M., Sun, J. Y., Wu, Z. J., Yue, D. L., Shen, X. J., Zhang, Y. M., Pei, X. Y., Cheng, Y. F., &
730 Wiedensohler, A. (2013). Characteristics of regional new particle formation in urban and
731 regional background environments in the North China Plain. *Atmospheric Chemistry and Physics*,
732 13(24), 12495–12506. <https://doi.org/10.5194/acp-13-12495-2013>
- 733 Wang, Z., Wu, Z., Yue, D., Shang, D., Guo, S., Sun, J., Ding, A., Wang, L., Jiang, J., Guo, H., Gao, J.,
734 Cheung, H. C., Morawska, L., Keywood, M., & Hu, M. (2017). New particle formation in China:
735 Current knowledge and further directions. *Science of the Total Environment*, 577, 258–266.
736 <https://doi.org/10.1016/j.scitotenv.2016.10.177>
- 737 Xiao, S., Wang, M. Y., Yao, L., Kulmala, M., Zhou, B., Yang, X., Chen, J. M., Wang, D. F., Fu, Q. Y.,
738 Worsnop, D. R., & Wang, L. (2015). Strong atmospheric new particle formation in winter in
739 urban Shanghai, China. *Atmospheric Chemistry and Physics*, 15(4), 1769–1781.
740 <https://doi.org/10.5194/acp-15-1769-2015>
- 741 Yan, C., Yin, R., Lu, Y., Dada, L., Yang, D., Fu, Y., Kontkanen, J., Deng, C., Garmash, O., Ruan, J.,
742 Baalbaki, R., Schervish, M., Cai, R., Bloss, M., Chan, T., Chen, T., Chen, Q., Chen, X., Chen, Y., ...
743 Bianchi, F. (2021). The Synergistic Role of Sulfuric Acid, Bases, and Oxidized Organics Governing
744 New-Particle Formation in Beijing. *Geophysical Research Letters*, 48(7), 1–12.
745 <https://doi.org/10.1029/2020GL091944>
- 746 Yang, L., Nie, W., Liu, Y., Xu, Z., Xiao, M., Qi, X., Li, Y., Wang, R., Zou, J., Paasonen, P., Yan, C., Xu, Z.,
747 Wang, J., Zhou, C., Yuan, J., Sun, J., Chi, X., Kerminen, V. M., Kulmala, M., & Ding, A. (2021).
748 Toward Building a Physical Proxy for Gas-Phase Sulfuric Acid Concentration Based on Its Budget
749 Analysis in Polluted Yangtze River Delta, East China. *Environmental Science and Technology*,
750 55(10), 6665–6676. <https://doi.org/10.1021/acs.est.1c00738>
- 751 Yao, L., Garmash, O., Bianchi, F., Zheng, J., Yan, C., Paasonen, P., Sipilä, M., Wang, M., Wang, X., &
752 Xiao, S. (2018). Atmospheric new particle formation from sulfuric acid and amines in a Chinese
753 megacity. *Science*, 281(July), 278–281.
- 754 Yu, H., Hallar, A. G., You, Y., Sedlacek, A., Springston, S., Kanawade, V. P., Lee, Y. N., Wang, J., Kuang,
755 C., McGraw, R. L., McCubbin, I., Mikkila, J., & Lee, S. H. (2014). Sub-3 nm particles observed at
756 the coastal and continental sites in the United States. *Journal of Geophysical Research*, 119(2),
757 860–879. <https://doi.org/10.1002/2013JD020841>
- 758 Yu, H., Ren, L., & Kanawade, V. P. (2017). New Particle Formation and Growth Mechanisms in Highly
759 Polluted Environments. *Current Pollution Reports*, 3(4), 245–253.
760 <https://doi.org/10.1007/s40726-017-0067-3>
- 761 Yue, D., Hu, M., Wu, Z., Wang, Z., Guo, S., Wehner, B., Nowak, A., Achtert, P., Wiedensohler, A., Jung,
762 J., Kim, Y. J., & Liu, S. (2009). Characteristics of aerosol size distributions and new particle
763 formation in the summer in Beijing. *Journal of Geophysical Research Atmospheres*, 114(14), 1–
764 13. <https://doi.org/10.1029/2008JD010894>



- 765 Zhang, R., Khalizov, A., Wang, L., Hu, M., & Xu, W. (2012). Nucleation and growth of nanoparticles in
766 the atmosphere. In *Chemical Reviews* (Vol. 112, Issue 3, pp. 1957–2011).
767 <https://doi.org/10.1021/cr2001756>
- 768 Zhang, R., Wang, G., Guo, S., Zamora, M. L., Ying, Q., Lin, Y., Wang, W., Hu, M., & Wang, Y. (2015).
769 Formation of Urban Fine Particulate Matter. *Chemical Reviews*, 115(10), 3803–3855.
770 <https://doi.org/10.1021/acs.chemrev.5b00067>
- 771 Zhang, Y., Tao, J., Ma, N., Kuang, Y., Wang, Z., Cheng, P., Xu, W., Yang, W., Zhang, S., Xiong, C., Dong,
772 W., Xie, L., Sun, Y., Fu, P., Zhou, G., Cheng, Y., & Su, H. (2020). Predicting cloud condensation
773 nuclei number concentration based on conventional measurements of aerosol properties in the
774 North China Plain. *Science of the Total Environment*, 719, 137473.
775 <https://doi.org/10.1016/j.scitotenv.2020.137473>
- 776 Zhou, Y., Dada, L., Liu, Y., Fu, Y., Kangasluoma, J., Chan, T., Yan, C., Chu, B., Daellenbach, K. R., Bianchi,
777 F., Kokkonen, T. V., Liu, Y., Kujansuu, J., Kerminen, V. M., Petäjä, T., Wang, L., Jiang, J., &
778 Kulmala, M. (2020). Variation of size-segregated particle number concentrations in wintertime
779 Beijing. *Atmospheric Chemistry and Physics*, 20(2), 1201–1216. [https://doi.org/10.5194/acp-20-](https://doi.org/10.5194/acp-20-1201-2020)
780 [1201-2020](https://doi.org/10.5194/acp-20-1201-2020)
- 781 Zhu, Y., Yan, C., Zhang, R., Wang, Z., Zheng, M., Gao, H., Gao, Y., & Yao, X. (2017). Simultaneous
782 measurements of new particle formation at 1s time resolution at a street site and a rooftop site.
783 *Atmospheric Chemistry and Physics*, 17(15), 9469–9484. [https://doi.org/10.5194/acp-17-9469-](https://doi.org/10.5194/acp-17-9469-2017)
784 [2017](https://doi.org/10.5194/acp-17-9469-2017)
785